An Approach for Reliable Calibrations of Ultra-high Value Resistors with the Dual Source Bridge

MAPAN-Journal of Metrology Society of India (June 2025) 40(2):547–555
https://doi.org/10.1007/s12647-025-00819-9

ORIGINAL PAPER

An Approach for Reliable Calibrations of Ultra-high Value Resistors with the Dual Source Bridge

I. Mihai and F. Galliana*

Department of Applied Metrology and Engineering, National Institute of Metrological Research (INRIM), Strada Delle Cacce 91, 10135 Turin, Italy

Received: 02 February 2025 / Accepted: 19 March 2025 / Published online: 8 May 2025

Abstract: At the Istituto Nazionale di Ricerca Metrologica (INRiM), an approach for reliably calibrating ultra-high-value resistors with the dual source bridge (DSB) is proposed as part of the INRiM knowledge transfer task. This approach is particularly suitable for commercial DSBs, which can be used by electrical calibration laboratories for their activities for external clients. The approach is based on ratio measurements, metrological triangulation rule and measurement compatibility. The proposed reliable calibration value is the corrected weighted mean of three intermediate calibration values which must satisfy a strict triangulation rule and be compatible within small uncertainties. This approach helps to reduce systematic errors or to include them into the uncertainty of the corrected weighted mean. For this paper the method was applied to three high value resistors using a commercial DSB to obtain a reliable calibration value of a 1 PΩ resistor. This technique meets the requirements of the EN 17025 standard for risk assessment of calibration activities.

Keywords: High resistance measurements; Measurement uncertainty; Systematic errors; Extrapolation; Weighted mean; Measurement compatibility

1. Introduction

Main errors of high and ultra-high electrical resistance measurements are due to the: drift, temperature and voltage dependence of the reference resistors, leakages, connections, sensitivity and resolution of measurement setups, temperature instability of resistors under calibration, loading effects, and stabilisation times. Additional errors that can occur with dual source bridges (DSBs) [1–5] include voltage calibrators instability, residual bridge balance current, electronic noise and voltage burden of the detector, offset and thermal voltages residual to polarity reversal. However, most National Measurement Institutes (NMIs) used the DSB method in the international comparisons [6, 7]. For commercial DSBs, such as those equipped with coaxial cables, leakage errors are probably not adequately minimised. Leakage resistances on the Hi side (R_x) of the measurement setup, which are in parallel with the low impedance of a calibrator, do not affect the measurements. In contrast, leakage resistances on the Lo side (R_s) affect the measurements by draining a small current, because it is not possible to achieve a perfect bridge balance. Effective methods to reduce the effects of leakages are described in [2, 8, 9]. Our approach is instead based on triangulation rules and measurement compatibility. It is focused on obtaining reliable calibration values for ultra-high resistances by identifying, correcting or delimiting systematic errors. The novelty of this work is to consider the corrected weighted mean of three intermediate calibration values as a reliable calibration value. The intermediate values must satisfy a strict triangulation rule and be compatible within small uncertainties [10]. This approach can reduce errors of the DSB method or include them into the uncertainty of the corrected weighted mean of the three intermediate calibration values. In addition, this technique can be used to calibrate the entire high-resistance scale and meets the requirements of [11] for risk assessment in calibration activities.

2. Measurements at the Istituto Nazionale di Ricerca Metrologica (INRiM)

For this study, the measurements were made in a shielded chamber, with temperature and relative humidity

*Corresponding author, E-mail: f.galliana@irim.it

controlled at (23 ± 0.5 °C and, 40 ± 10) % respectively. High humidity has an unwanted effect on high value resistances because it lowers their values and this effect lasts for at least two weeks even after moving the resistors to a drier environment. In our case, humidity is maintained at the level typical of electrical calibration laboratories and measurements lasting over a period of weeks allow to eliminate any inertia in the resistors values for humidity effects. The measurements were performed by means of the circuit of Fig. 1. All the shields of the resistors, cables and connectors are connected to the low terminal of the detector that is also rear connected to its ground terminal. This point, to which all shields are connected, is further connected to an independent ground potential of the laboratory, disconnected from the ground potential of the mains to avoid noises. The measurements were performed with the INRiM commercial DSB that is equipped with coaxial cables. The ratio values in ppm from the measurement system are given by the bridge software in comparison with the reference values entered by the operator when programming the measurement.

The multiple measurements mode [12] was used, which consists of automatic measurement steps in which the value of the resistor under calibration (R_x) is updated at each step. This process progressively reduces the bridge unbalance and the current at the detector, approaching the ideal balance. In [13], it was observed that the ratio measurements at the third step were approximately normally distributed, with the lowest standard deviation of the mean [10] among all steps. In [13, 14] it is shown that in the first two measurement steps, transient effects due to electronic noises of the measurement system were still present and the bridge stabilization period was not yet completed, resulting in high standard deviations of the measurements. From the fourth step onwards, further unwanted effects such as drift of the calibrators were observed. In addition, a compatibility test showed that at the third step the bridge measurements were compatible with the reference measurements [14]. The noise at the detector was also investigated to determine the optimum number of readings required to carry out measurements in the white noise regime, where the classical variance can be applied [14, 15]. Errors of the voltage calibrators were further minimised by calibrating them prior to the measurements. The bridge software uses the calibration results of the calibrators to correct their output voltages in subsequent

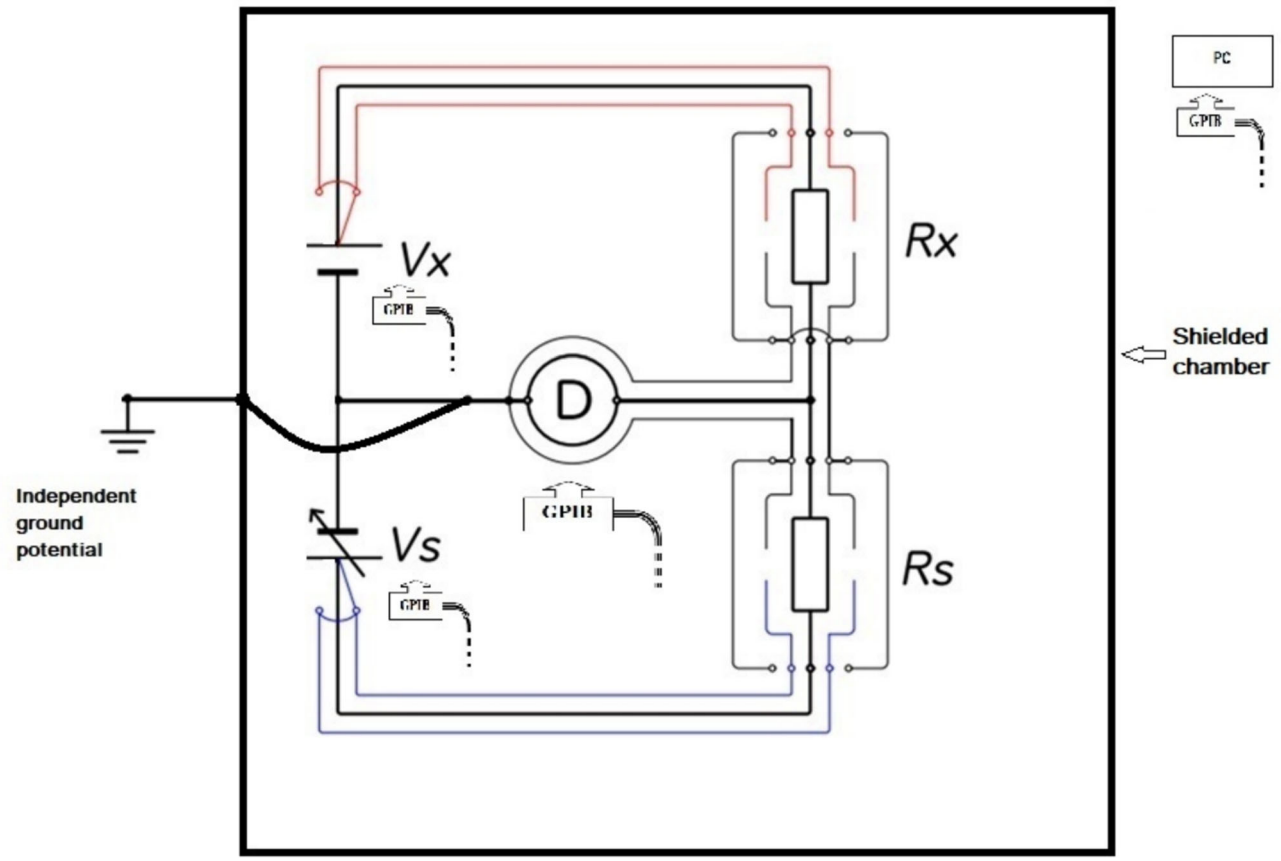

Fig. 1 Simplified scheme of the INRiM measurement system based on the commercial DSB controlled by a pc outside the shielded chamber to eliminate its noise

calibrations [12]. As the resistors under comparison were placed in a thermally controlled air bath at (23 ± 0.1)°C, thermal voltages residual to polarity reversal and temperature effects were minimised. The ratio measurements r_E, r_A, and r_G were performed with the INRiM commercial DSB on a 10 TΩ, a 100 TΩ and a 1 PΩ resistors at 500 V, 750 V, and 1000 V, following the triangular scheme shown in Fig. 2. The proposed approach was applied to calibrate the 1 PΩ resistor.

The resistors used are listed in Table 1. The MI[1] resistor is based on a bulk resistive element, while the Gdl[2] resistors are based on resistive networks. The 100 TΩ resistor, with a flat voltage coefficient, was one of the travelling resistors of the comparison [7].

The measurements were performed at the time constant of the 10 TΩ resistor, (280 s).

2.1. Extrapolation of the 10 TΩ Values at Low Voltages

The 10 TΩ resistor, as reference resistor R_s, has been previously calibrated at 250 V, 500 V, 750 V and 1000 V[3]F with the INRiM DSB [3, 5], validated by its successful participation at the comparison [7]. As the sensitivity limit of the DSB detectors does not always allow the correct calibration of ultra-high resistors at low voltages, the values of the 10 TΩ resistor at low voltages, were extrapolated using the INRiM Calibration Curves Computing (CCC) software [16, 17]. This software, which is suitable for fitting correlated data, has been used since a correlation among the extrapolated values exists for the voltage coefficient of the resistor. A second order polynomial has been chosen:

$$(R_s(V) - R_{nom})/R_{nom} = a + bV + cV^2 \quad (1)$$

where R_{nom} is the nominal value of the resistor, while b and c are its voltage coefficients.

The combined standard uncertainty of R_s (10 TΩ) DSB. The application range of Eq. (1) is from 0 to 100 V in our case. However, the CCC software provides several alternative matching solutions for any voltage range. The application range of Eq. (1) depends on the voltages at which the resistor has been previously calibrated and applies to the voltages below the lowest voltage at which the resistor has been calibrated.

2.2. Distribution of the Ratio Measurements at the Step 3

Also in this case, the ratio measurements r_A, r_G and r_E at the third step were approximately normally distributed. Figures 4, 5, 6 and 7 show some histograms of the measurements fitted with the Stable32 software [18].

A normality analysis of the measurements at the step 3 has been also made using the R software [19] at a 95% confidence level. A p-value higher than 0.05 supports the hypothesis that the data follow a normal distribution. The results in Table 2 show that all the data sets conform to a Gaussian distribution. Figure 8 shows a histogram with the R software.

3. Steps of the Proposed Approach

Figure 9 shows a flow chart of the approach that is explained in detail after Fig. 9.

The approach consists in the following steps:

Determination of two 1 PΩ values, a ccording to the scheme in Fig. 2, via a 1:100 and two 1:10 ratios respectively:

$$1\ \mathrm{P\Omega}_{rE} = 10\ \mathrm{T\Omega} \times r_E \quad (3)$$

$$1\ \mathrm{P\Omega}_{rAG} = 10\ \mathrm{T\Omega} \times r_A \times r_G \quad (4)$$

Verification of the metrological acceptability of the extrapolation of the 10 TΩ values at low voltages. To achieve this, a strict triangulation rule has to be applied:

$$u_{R_s} = \sqrt[2]{(u_c)^2 \cdot V^4 + (u_b)^2 \cdot V^2 + (u_a)^2 + 2 \cdot (u_{b,c}) \cdot V^3 + 2 \cdot (u_{a,c}) \cdot V^2 + 2 \cdot (u_{a,b}) \cdot V + u_{IB}^2} \quad (2)$$

is:where u_a, u_b, u_c are the uncertainties of the fit parameters while u_{ba}, u_{ac}, u_{bc} are their covariances. u_{iB} is the standard uncertainty of the 10 TΩ values calibrated with the INRiM

$$\overline{r_E} \cong \overline{r_A} \times \overline{r_G} \text{ or } 1 - \frac{r_A \times r_G}{r_E} \times 10^6 \cong 0 \quad (5)$$

The acceptability limit of Eq. (5) is defined as:

$$1 - \frac{r_A \times r_G}{r_E} \times 10^6 < \sqrt{s_{rA}^2 + s_{rG}^2 + s_{rE}^2} \quad (6)$$

[Par6] Measurement International (MI).

[Par7] Guildline (Gdl).

[Par10] The INRiM Calibration Measurement Capability (CMC) at 10 TΩ is valid for voltages between 500 and 1000 V.

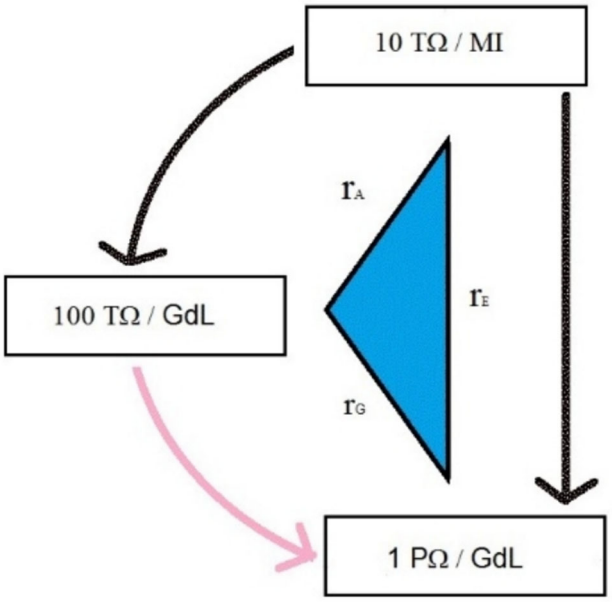

Fig. 2 The ratio measurements

Table 1 Resistors used in the measurements

Resistor	Serial no	Model
10 TΩ	1,101,167	MI 9331G/10TΩ
100 TΩ	69,640	Gdl 9337-100 T
1 PΩ	72,587	Gdl 9337-1P

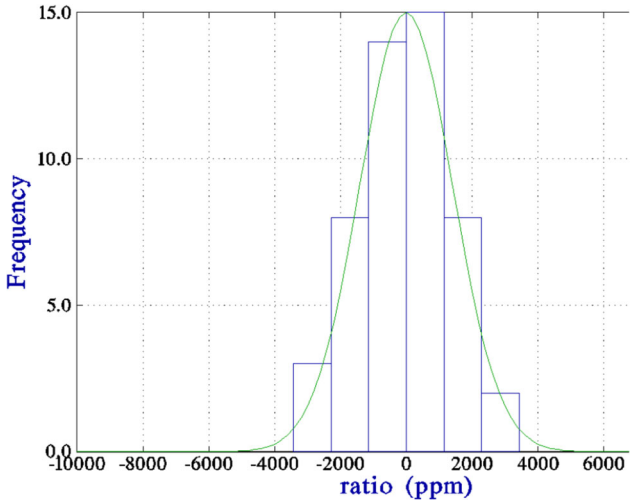

Fig. 4 r_A measurements at the step3 at 500 V

where s_{rA}, s_{rG}, s_{rE} are the lowest standard deviations of the mean of the ratio measurements at the third step of the measurements. Table 3 shows the results of Eq. (6) where it can be seen that the established rule in this case is satisfied for all voltages in our case. This means that the extrapolation has been acceptable for the purpose and with respect to the overall measurement uncertainty at 1 PΩ level;

Measurement of the ratio $r_{A\_50\text{-}75\text{-}100V}$ at 50 V, 75 V and 100 V, using the values extrapolated at 5 V, 7.5 V and 10 V of the 10 TΩ already utilised for r_E:

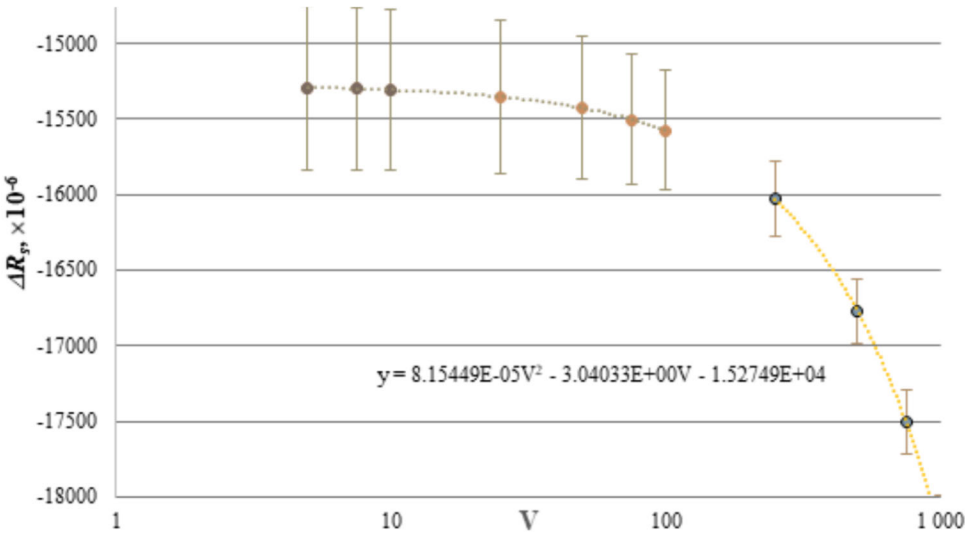

Fig. 3 Fitting curve with the CCC software for the 10 TΩ resistor. The calibration and extrapolated values (the latter ranging from 5 to 100 V) are represented by the yellow and brown lines, respectively along with their uncertainties at k = 1 [10]. Voltages are shown on a logarithmic scale (Fig. 3)

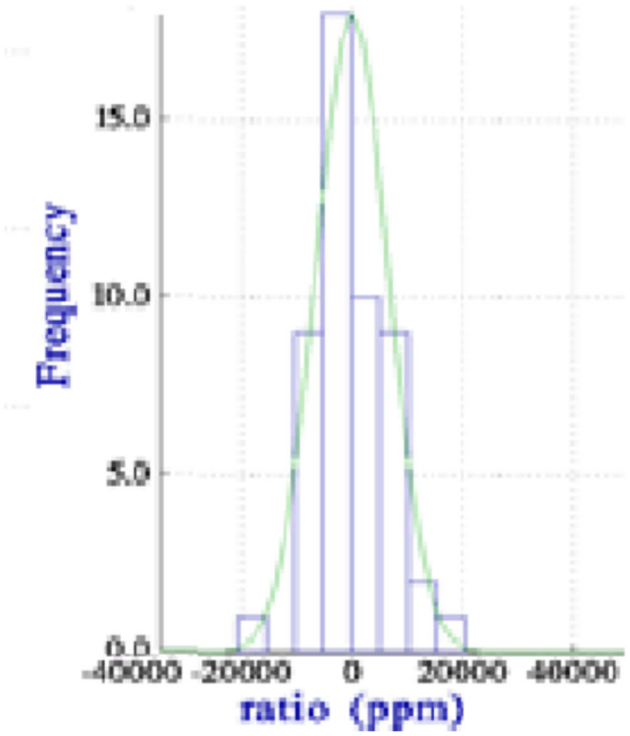

Fig. 5 r_E measurements at the step3 at 1000 V

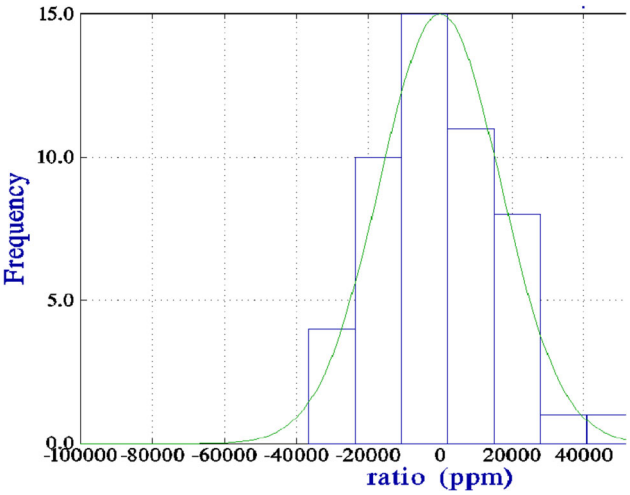

Fig. 6 r_G measurements at step3 at 500 V

$$r_{A\_50-75-100\mathrm{V}} \cong r_{A'\_50-75-100\mathrm{V}} e \tag{7}$$

where ε is the $r_{A'}$ error.[4] Since r_E suffers from an error of the same order, it can be:

$$r_E \cong r_{E\_500-750-1000\mathrm{V}} e \tag{8}$$

and

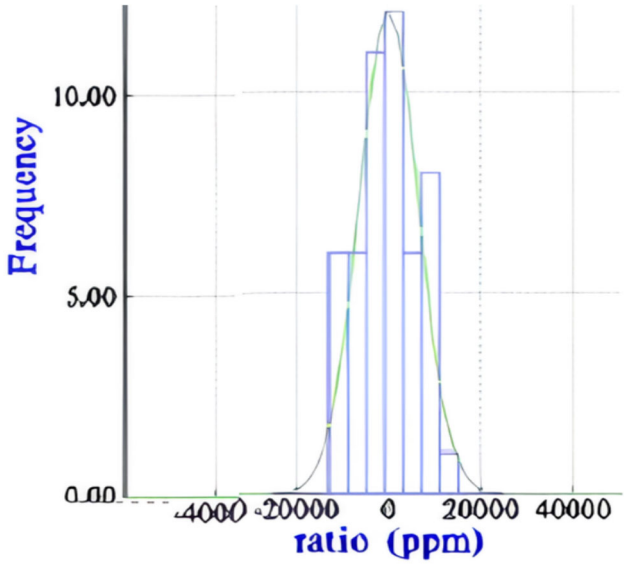

Fig. 7 r_G measurements at step3 at 1000 V

$$1\ \mathrm{P\Omega}_{rE} = 10\ \mathrm{T\Omega} \times r_E e \tag{9}$$

From (8) and (7):

$$r_{G'} = r_{E\_500-750-1000\mathrm{V}} e / r_{A'\_50-75-100\mathrm{V}} e \tag{10}$$

therefore $r_{G'}$ is not affected by the error ε

$$1\ \mathrm{P\Omega}_{rAG'} = 10\ \mathrm{T\Omega} \times r_A e \times r_{G'} \tag{11}$$

The error ε instead affects 1 $\mathrm{P\Omega}_{rAG}$ and 1 $\mathrm{P\Omega}_{rE}$.

Verification of the mutual compatibility among 1 $\mathrm{P\Omega}_{r,E}$ $\mathrm{P\Omega}_{rAG}$ and 1 $\mathrm{P\Omega}_{rAG'}$ considering the standard deviations of the mean of r_E, r_{AG} and $r_{AG'}$ at the step 3 as their respective uncertainties;

Calculation of the Weighted mean 1 $\mathrm{P\Omega}_{wm}$ of the three 1 PΩ values if the conditions of the steps 2 and 4 are satisfied.

Correction of 1 $\mathrm{P\Omega}_{wm}$ using the ratio values between 1 $\mathrm{P\Omega}_{r,E}$ Eq. (9) and 1 $\mathrm{P\Omega}_{rAG}$ Eq. (11) where ε is cancelled.[5] Corrected weighted mean 1 $\mathrm{P\Omega}_{cwm}$ as reliable calibration value of 1 PΩ.

This procedure minimises errors or includes them into the uncertainty of 1 $\mathrm{P\Omega}_{cwm}$.

4. Compatibility Check at 1 PΩ

Table 4 reports the ratios and the corresponding 1 PΩ values at the third step of the measurements, along with their standard deviations of the mean s at the same step. Table 5 reports the mutual relative differences among the 1

Par20 Mainly due to the leakages and to the extrapolation of the 10 TΩ values at low voltages. Effects of other errors have to be considered in the type B uncertainty evaluation [10].

Par26 This correction removes ε in the corrected weighted mean but errors coming from 1 $\mathrm{P\Omega}_{rAG}$ remain. Their effects are however minimised since enclosed in 1 $\mathrm{P\Omega}_{cwm}$.

Table 2 Normality test for each ratio measurement at the step3

Dataset	Mean (μΩ/Ω)	Standard deviation of the mean (μΩ/Ω)	W	*p*-value	Distribution
r_G_500V	8826.5	2374.5	0.98	0.78	Normal
r_G _750V	6177.7	1291.8	0.98	0.6	Normal
r_G _1000V	6854.9	912.5	0.97	0.3	Normal
r_E _500V	27,177.7	1654.0	0.99	0.9	Normal
r_E 750 V	24,379	1087.5	0.98	0.6	Normal
r_E _1000V	23,835.6	923.6	0.98	0.8	Normal
r_A _500V	17,432.9	199.3	0.98	0.8	Normal
r_A _750V	17,642.1	153.5	0.97	0.2	Normal
r_A _1000V	17,820.7	97.5	0.97	0.2	Normal

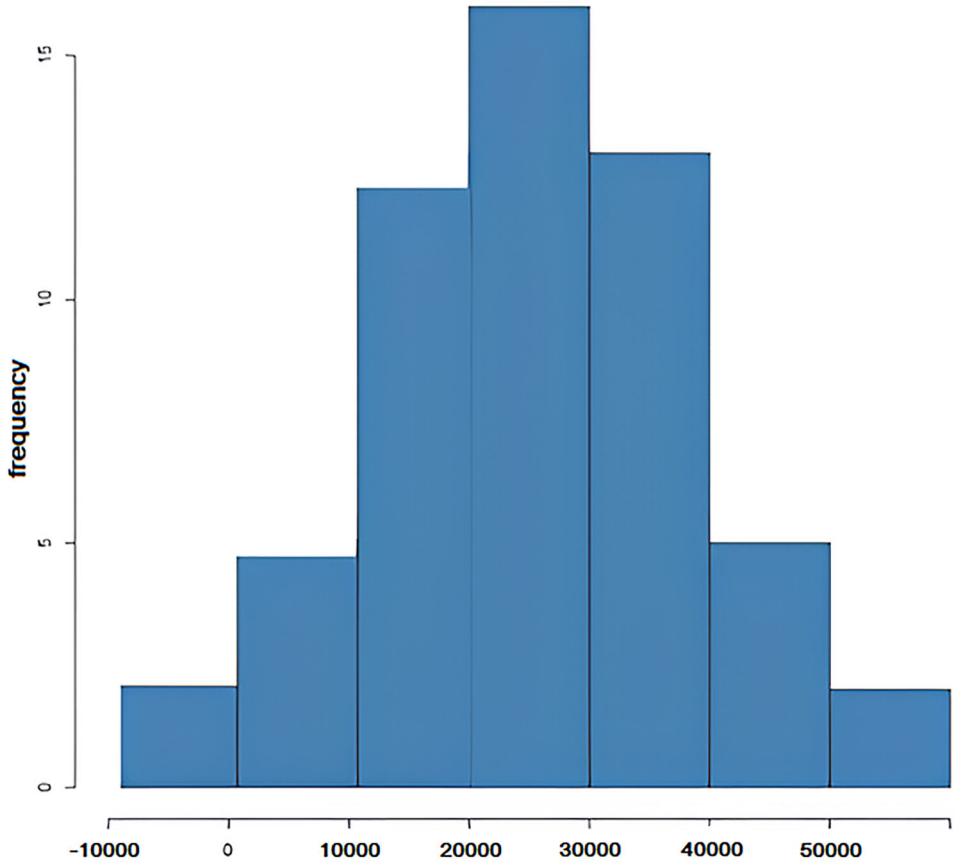

Fig. 8 Histogram of r_G at step3 at 500 V with the R software

PΩ values, the uncertainties (k = 1) of these differences, and the normalised errors, as defined by [20]. In these uncertainties, a correlation term for the common 10 TΩ resistor has been included. The results in Table 5 show that in the presented case there is satisfactory mutual compatibility between the intermediate values of 1 PΩ, since all the normalised errors are less than |0.5|. Table 6 gives the ratio values between 1 $P\Omega_{r,E}$ and 1 $P\Omega_{rAG'}$ along with the corresponding correction values of 1 $P\Omega_{wm}$. Table 7 reports the values of 1 $P\Omega_{cwm}$ and their uncertainties (k = 1) where the same correlation term has been considered.

Finally, Fig. 10 shows graphically the compatibilities among the 1 PΩ values and their corrected weighted mean.

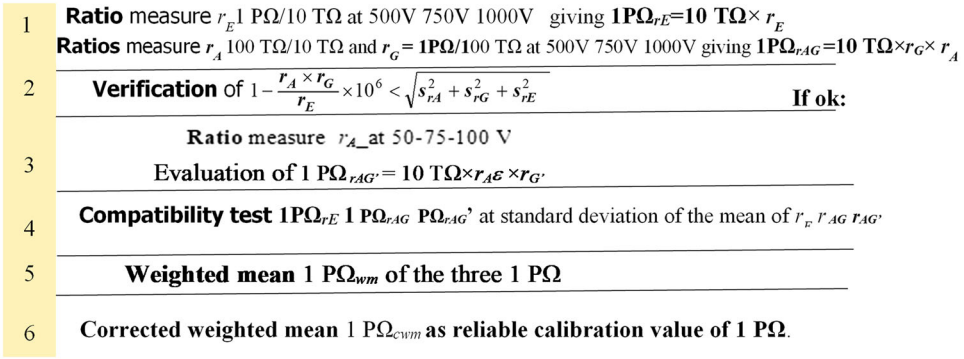

Fig. 9 Flow chart of the steps of the proposed approach

Table 3 Absolute values of the Eq. (6a and b) at the step3 of the ratio measurements

Settle-time Step 3 (s)	Voltage (V)	Equation (6)	
		a ($\times 10^{-6}$)	b ($\times 10^{-6}$)
1120	500	822	2906
1120	750	439	1696
1120	1000	940	1302

A satisfactory agreement was achieved among 1 PΩ$_{rE}$, 1 PΩ$_{rAG}$, and 1 PΩ $_{rAG'}$ and their corrected weighted mean. This result is promising, since the compatibility test was carried out under restrictive conditions.

5. Discussion

This paper presents an approach for reliable calibrations in the field of ultra-high electrical resistance, specifically using the DSB, including commercial versions. For each decade of a high resistance scale, the weighted mean of three intermediate calibration values has to be calculated. The first intermediate value comes from a direct 1:100 ratio, the second from two 1:10 ratios, and the third from a calculated ratio. The first two intermediate values must satisfy a strict triangulation rule and all the three intermediate values must be mutually compatible within their standard deviations of the mean. The weighted mean of these three intermediate values can be corrected with simple calculations and can represent a reliable calibration value for ultra-high value resistors. Although the process may seem complex and time-consuming because it usually takes days to complete, it can be speeded up by using automated techniques and high-resistance scanners, thus taking advantage of measurements during nights or weekend. This approach minimises systematic errors that affect the DSB method or includes them into the uncertainty of the corrected weighted mean. A limitation of the approach is the extrapolation of the values of the reference resistor at low voltages due to the sensitivity limit of DSBs detectors. Methods using precise small current generation and measurement [21–23] could overcome this limitation. The proposed approach allows the use of commercial DSBs at very small uncertainties typical of NMIs or high-end secondary laboratories. These laboratories are gradually replacing the DSB method with others based on the Ultrastable low-noise current amplifier (ULCA). However, for repetitive measurements (e.g. annually calibrations), the complete approach can be applied only when a new resistor

Table 4 Values of the ratios and of the corresponding 1 PΩ with their standard deviations of the mean at the step 3

Voltage (V)	r_E	1 PΩ$_{rE}$ (PΩ)	s(1 PΩ$_{rE}$) ($\times 10^{-6}$)	r_{AG}	1 PΩ$_{rAG}$ (PΩ)	s(1 PΩ$_{rAG}$) ($\times 10^{-6}$)	$r_{AG'}$	1 PΩ$_{rAG'}$ (PΩ)	s(1 PΩ$_{rAG'}$) ($\times 10^{-6}$)
500	102.718	1.0115	1655	102.633	1.0105	2388	101.025	1.0106	2038
750	102.438	1.0087	1087	102.393	1.0088	1301	100.734	1.0090	1304
1000	102.384	1.0082	924	102.479	1.0081	918	100.269	1.0085	1093

Table 5 Mutual compatibility checks among 1 $P\Omega_{rE}$ 1 $P\Omega_{rAG,}$ and 1 $P\Omega_{rAG'}$

Voltage (V)	$\Delta_{(1P\Omega rE\text{-}1P\Omega rAG)}$ ($\times 10^{-6}$)	$u(\Delta_{1P\Omega rE\text{-}1P\Omega rAG})$ ($\times 10^{-6}$)	$E_{n\ 1\ P\Omega rE\text{-}1P\Omega rAG}$	$\Delta_{(1P\Omega rE\text{-}1P\Omega rAG')}$ ($\times 10^{-6}$)	$u(\Delta_{(1P\Omega rE\text{-}1P\Omega rAG')})$ ($\times 10^{-6}$)	$E_{n\ 1\ P\Omega rE\text{-}1P\Omega rAG'}$	$\Delta_{(1P\Omega rAG\text{-}1P\Omega rAG')}$ ($\times 10^{-6}$)	$u(\Delta_{(1P\Omega rAG\text{-}1P\Omega rAG')})$ ($\times 10^{-6}$)	$E_{n\ 1\ P\Omega rAG\text{-}1\ P\Omega rAG'}$
500	972.7	2787	0.3	868.1	2494	0.3	−104.6	3031	−0.03
750	−119.7	1503	−0.1	−319.4	1506	−0.2	−199.6	1667	−0.1
1000	110.1	1051	0.1	868.1	2494	0.3	−460.0	1202	−0.4

Table 6 Ratio values between 1 $P\Omega_{rE}$ and 1 $P\Omega_{rAG'}$ and correction values of the weighted mean

Voltage (V)	1 $P\Omega_{rE}$/1 $P\Omega_{rAG'}$	Correction values ($\times 10^{-6}$)
500	1.000859	859
750	0.999683	−317
1000	0.999653	−347

Table 7 Corrected weighted mean (expressed as relative deviation from nominal value) of 1 $P\Omega_{rE}$, 1 $P\Omega_{rAG,}$ and 1 $P\Omega_{rAG'}$ and its uncertainty ($k = 1$)

Voltage (V)	$1P\Omega_{cwm}$ ($\times 10^{-6}$)	$u(1P\Omega_{cwm})$ ($\times 10^{-6}$)
500	10,128	1522
750	9152	1217
1000	8564	1146

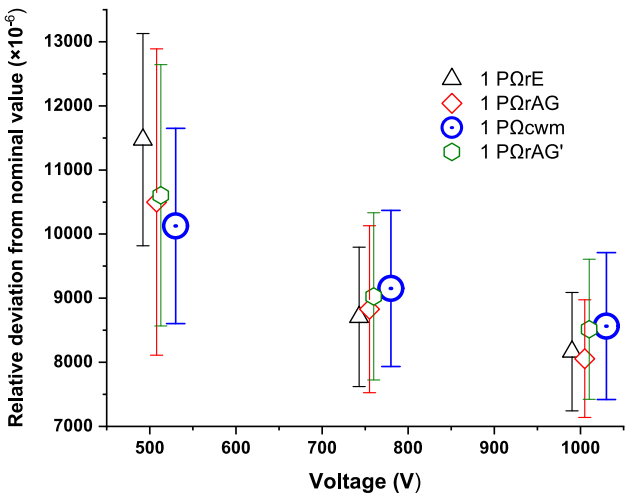

Fig. 10 Compatibility at $k = 1$ confidence level among 1 $P\Omega_{rE}$, 1 $P\Omega_{rAG}$, 1 $P\Omega_{rAG'}$ and their corrected weighted mean 1 $P\Omega_{cwm}$ (expressed as relative deviation from nominal value). The uncertainty bars correspond to the standard deviations of the mean

has to be calibrated. After the first calibration, only one of the three intermediate values can be used as calibration value in the successive calibrations, thus considerably easing the procedure. The same applies if a laboratory does not need particularly small uncertainties as industrial laboratories. Laboratories still equipped with commercial DSBs could perform internal costs-benefits analysis according to their needs between still using the DSB combined with this approach or purchasing more advanced instrumentation now available in this measurement field. However, it is recommended to carefully read the uncertainty specification of instruments claiming better performance, as some uncertainty contributions may be excluded from the specifications for commercial reasons. Future work will include a full validation of the approach through a compatibility test at 1 PΩ, comparing the INRiM result with that of the Laboratoire National de Métrologie et d'Essais (LNE, France). The LNE method for ultra-high resistance measurements consists of an integration technique that improves the capacitor charging method (CCA) [24, 25]. The Calibration and Measurement Capability (CMC) at 1 PΩ of the LNE is recognised by the Mutual Recognition Arrangement (MRA).[6] A collaboration on this subject between INRIM and LNE is underway. Another possible outcome should be the replacement of the detector

Par32 The CIPM Mutual Recognition Arrangement (CIPM MRA) is an agreement among National Metrology Institutes to demonstrate the international equivalence of their measurement standards and the calibration and measurement certificates they issue. The outcomes of the Arrangement are the internationally recognized (peer-reviewed and approved) Calibration and Measurement Capabilities (CMCs) of the participating institutes.

of the INRiM's commercial DSB with a more sensitive one.

Declarations

Conflict of interest The authors declare they have no conflicts of interest with the instrumentation manufacturers. The research was funded on INRIM funds. Measurement data are available at https://zenodo.org/uploads/14356308.

References

1. L.C.A. Henderson, A new technique for the automatic measurement of high value resistors. J. Phys. E. Sci. Instrum., *20* (1987) 492–495.
2. D.G. Jarrett, Automated guarded bridge for calibration of multimegohm standard resistors from 1 MΩ to 1 TΩ. IEEE Trans. Instrum. Meas., *46*(2) (1997) 325–328.
3. F. Galliana, P.P. Capra and E. Gasparotto, Evaluation of two alternative methods to calibrate ultra–high value resistors at INRIM. IEEE Trans. Meas., *60*(3) (2011) 965–970.
4. I. Leniček, D. Ilić and L. Ferković, High value resistance comparison using modified Wheatstone bridge based on current detection. Measurement, *46*(10) (2013) 4388–4393. https://doi.org/10.1016/j.measurement.2013.05.018.
5. F. Galliana and G. Boella, The electrical DC resistance scale from 100 kΩ to 1 TΩ at IEN IEEE Trans. Instrum. Meas., *49*(5) (2000) 959–963. https://doi.org/10.1109/19.872914.
6. R.F. Dziuba and D.G. Jarrett, Final report on key comparison CCEM–K2 of resistance standards at 10 MΩ and 1 GΩ, 002. Metrologia, *39* (2001) 01001. https://doi.org/10.1088/0026-1394/39/1A/1.
7. B. Jeckelmann, J.H.N. van der Beek, P.P. Capra, P. Chrobok, L. Cirneanu, E. Dudek and P. Vrabcek, Final report on supplementary comparison EURAMET. EM-S32: comparison of resistance standards at 1 TΩ and 100 TΩ. Metrologia, *50*(1A) (2013) 01008–01008.
8. K.M. Yu, W.S. Kim, S.H. Lee, K.S. Han and J.H. Kang, A method for measuring high resistances with negligible leakage effect using one voltage source and one voltmeter. Meas. Sci. Technol., *25*(7) (2014) 075012.
9. R.E. Elmquist et al, NIST Technical Note 1458. (2003)
10. JCGM 100:2008 Evaluation of measurement data – Guide to the expression of uncertainty in measurement First edition
11. ISO/IEC 17025 General requirements for the competence of testing and calibration laboratories, 3rd edition, February (2018)
12. Measurement International 2013 automated dual source high resistance bridge mod. 6600A, operator manual, rev. 2
13. I. Mihai and F. Galliana, Application of statistical tools to optimize a dual source electrical high DC resistance bridge. MAPAN-J. Metrol. Soc India, *38*(3) (2023) 573–581. https://doi.org/10.1007/s12647-023-00665-7.
14. I. Mihai, P.P. Capra and F. Galliana, Evaluation of a commercial high resistance bridge and methods to improve its precision. Metrol. Mea. Syst., *29*(4) (2022) 701–718.
15. D.W. Allan, Should the classical variance be used as a basic measure in standards metrology? IEEE Trans. Instrum. Meas., *IM–36* (1987) 646–654.
16. A. Malengo and F. Pennecchi, A weighted total least–squares algorithm for any fitting model with correlated variables. Metrogia, *50* (2013) 654–662.
17. Calibration Curves Computing – CCC Software User manual 1.3 https://www.inrim.it/it/servizi/software-e-database/ccc-software
18. Hamilton Technical Services Stable32 User Manual, (2008) http://www.stable32.com
19. R Core Team 2022. R: A language and environment for statistical computing. R Foundation for Statistical Computing, Wien https://www.R-project.org/
20. ISO/IEC 17043:2023 Conformity assessment — General requirements for the competence of proficiency testing providers, Edition 2
21. N.-H. Kaneko, T. Tanaka and Y. Okazaki, Perspectives of the generation and measurement of small electric currents. Meas. Sci. Technol., *35* (2024) 011001. https://doi.org/10.1088/1361-6501/ad03a2.
22. L. Callegaro, C. Cassiago, V. D'Elia, E. Gasparotto, E. Enrico and M. Gotz, Comparison of low DC current traceability methods and gas capacitors AC–DC dependence. IEEE Trans. Instrum. Meas., *70* (2021) 1–6. https://doi.org/10.1109/TIM.2021.3053974 .
23. D. Drung, C. Krause, U. Becker, H. Scherer and F.J. Ahlers, Ultrastable low-noise current amplifier: a novel device for measuring small electric currents with high accuracy. Rev. Sci. Instrum. (2015). https://doi.org/10.1063/1.4907358.
24. S.H. Tsao, An accurate, semiautomatic technique of measuring high resistances. IEEE Trans. Instrum. Meas., *16*(3) (1967) 220.
25. E. Turhan, Ö. Erkan, C. Hayirli, D. Istrate, T. Németh, O. Power and D. Corminboeuf, EURAMET. EM-S44 comparison for ultra-low DC current sources. Metrologia, *60* (2023) 01002. https://doi.org/10.1088/0026-1394/60/1A/01002.